



Group Paging Mechanism with Pre-backoff for Machine-Type Communication

Yong Liu^(✉), Qinghua Zhu, Jingya Zhao, and Wei Han

School of Telecommunication Engineering, Beijing Polytechnic, Beijing 100176, China
liot.07@163.com

Abstract. In order to resolve congestion of the random access channel (RAC) caused by UE's concentrated access to the network in the process of group paging, this paper introduces the pre-backoff algorithm on the basis of studying MTC service characteristics to the group paging mechanism, and proposes the analysis model based on the group paging mechanism with pre-backoff. In the group paging mechanism with pre-backoff, when monitoring results indicate ongoing of group paging, all UE within the group, before access, will implement pre-backoff, and through pre-backoff, different pieces of UE are evenly distributed to a period of access time to alleviate collisions and conflicts resulted from concentrated access. Simulation results of three performance indexes, including the probability of conflict, probability of successful access and delay of average access, are used to analyze and verify the validity of the analysis model based on the group paging mechanism with pre-backoff.

Keywords: Machine-Type Communication (MTC) · Random Access Channel (RAC) · Group paging · Pre-backoff

1 Introduction

As the most important application form of the Internet of Things (IoT) for the time being, Machine-type Communications or MTC for short has brilliant application prospects and tremendous market potential [1]. Also known as Machine-to-Machine (M2M), MTC has been widely explored and implemented by three major telecommunications service providers in China, which has helped promote the MTC service development layout [2]. Nevertheless, the current Long-term Evolution (LTE) system, a primary supporting technology of MTC, for commercial use, which was initially designed to meet the needs of Human-type Communications (HTC), has failed to take the mass equipment and emergencies of MTC into consideration. As a result, when a large number of MTC terminals are switched into the LTE system designed on the basis of Human-to-Human (H2H) communications rules, access congestion would be inevitable. Therefore, it is of vital significance to improve the LTE mobile network to suit the application and development of MTC.

Though research into the MTC technology has been a general research interest, research findings are still limited. Apart from defining MTC service requirements and

functional structure based on the 3GPP standards, most researchers concentrate on studying the realization of application technologies, system structures and communication plans but pay little attention to the M2M service modeling and analysis [4]. The traditional mobile cellular network was originated from H2H communications, and has kept on evolving and improving according to user demands. Different from H2H communications, MTC is characterized by a high synchronicity of data transmission, low mobility of terminals, high terminal distribution density, etc.

Literature [5] points out that, in receiving group paging information, all user equipment (UE) immediately transmits its paging response through the random-access channel (RACH). Simultaneous signal access of all UE might result in serious conflicts of the RACH within a short period of time. Therefore, this paper, through introduction of the pre-backoff algorithm, puts forward an analysis model based on the pre-backoff group paging mechanism under MTC, attempting to address competition conflicts caused by users' concentrated access to the network and meet users' demand for quality of service (QoS).

2 Pre-backoff Group Paging Mechanism Analysis Model

This paper puts forward an analysis model based on the pre-backoff group paging mechanism, which can be used to analyze the performance of group paging strategies based on the pre-backoff algorithm. Three performance indexes, including probability of conflict (P_C), probability of successful access (P_S) and delay of average access (D_A) are employed to verify the accuracy and effectiveness of the pre-backoff group paging mechanism. The method proposed by this paper is not a process of repeated paging but makes use of the pre-backoff mechanism to expand the transmission of the first preamble to increase the probability of success at a lower access delay.

In the pre-backoff group paging mechanism, every UE should implement pre-backoff of its first transmission, and adheres to and supports random access of the repeatedly-transmitted standard LTE. The pre-backoff timer will evenly choose within the scope from 0 to W_{PBO} .

First of all, the pre-backoff group paging is available at the group paging interval of the I_{\max} -th RA (Random Access) timeslot. The group paging interval starts from and ends with the first RA timeslot. The pre-backoff algorithm can delay the first preamble transmission time to the pre-backoff window, W_{PBO} . The group paging is presented in Eq. (1). The definitions of various parameters are provided by Literature [6].

$$I_{\max} = \left\lceil \frac{W_{PBO}}{T_{RA_REP}} \right\rceil + 1 + (N_{PT\ max} - 1) \left\lceil \frac{(T_{RAR} + W_{RAR} + W_{BO})}{T_{RA_REP}} \right\rceil \quad (1)$$

Define $M_{i,S}[n]$ and $M_{i,F}[n]$ as the number of UE succeeding in transmitting and failing to send the n -th preamble at the i -th RA timeslot, respectively; $M_i[n]$ as the total number of UE transmitting the preamble at the i -th RA timeslot; P_P as the probability of the UE successfully receiving the paging information. After the paging information is received, " $P_P \times M$ " UE will immediately implement even backoff before transmitting

the first preamble. Export the total number of UE transmitting the first preamble at the i -th RA timeslot, $M_i [1]$, from Eq. (2).

$$M_i [1] = \begin{cases} \frac{P_p M}{W_{PBO}} & \text{if } i = 1 \\ \frac{T_{RA_REP} P_p M}{W_{PBO}} & \text{if } 2 \leq i \leq \left\lfloor \frac{W_{PBO}}{T_{RA_REP}} \right\rfloor \\ \frac{(W_{PBO} \bmod T_{RA_REP}) P_p M}{W_{PBO}} & \text{if } i = \left\lfloor \frac{W_{PBO}}{T_{RA_REP}} \right\rfloor + 1 \\ 0 & \text{otherwise} \end{cases} \quad (2)$$

There is no preamble retransmission in the first RA timeslot, so RA in the first RA timeslot tries to be investigated respectively with other RA timeslots. The number of successful UE, $M_{1,S}[n]$, UE in fault and $M_{1,F}[n]$ of the first RA timeslot are given by Eq. (3) and Eq. (4), respectively. Of special note is that, under the initial condition of $i = 1$, if $n \neq 1$, then $M_1[n] = 0$.

$$M_{1,S}[n] = \begin{cases} N_{UL} & \text{if } n = 1 \text{ and } M_i [1] e^{-\frac{M_i [1]}{R}} p_1 \geq N_{UL} \\ M_i [1] e^{-\frac{M_i [1]}{R}} p_1 & \text{if } n = 1 \text{ and } M_i [1] e^{-\frac{M_i [1]}{R}} p_1 < N_{UL} \\ 0 & \text{if } n \neq 1 \end{cases} \quad (3)$$

$$M_{1,F}[n] = \begin{cases} M_i [1] - N_{UL} & \text{if } n = 1 \text{ and } M_i [1] e^{-\frac{M_i [1]}{R}} p_1 \geq N_{UL} \\ M_i [1] (1 - e^{-\frac{M_i [1]}{R}} p_1) & \text{if } n = 1 \text{ and } M_i [1] e^{-\frac{M_i [1]}{R}} p_1 < N_{UL} \\ 0 & \text{if } n \neq 1 \end{cases} \quad (4)$$

Where, N_{UL} denotes the maximum number of UE which can be confirmed in the response window; p_n denotes the detection probability of the n preamble transmission under the power slope effect [7], and $p_n = 1 - (1/e^n)$; the UE failing at the first RA timeslot will implement backoff and be resent in the following RA timeslot. The total number of UE succeeding and failing at every RA timeslot, namely $M_{i,S}[n]$ and $M_{i,F}[n]$, can be respectively given by Eq. (5) and Eq. (6) recursively:

$$M_{1,S}[n] = \begin{cases} M_i [n] e^{-\frac{M_i [n]}{R}} p_n & \text{if } \sum_{n=1}^{N_{PT\max}} M_i [n] e^{-\frac{M_i [n]}{R}} p_n \leq N_{UL} \\ \frac{M_i [n] e^{-\frac{M_i [n]}{R}} p_n}{\sum_{n=1}^{N_{PT\max}} M_i [n] e^{-\frac{M_i [n]}{R}} p_n} & \text{otherwise} \end{cases} \quad (5)$$

$$M_{1,F}[n] = \begin{cases} M_i[n](1 - e^{-\frac{M_i}{R} p_n}) & \text{if } \sum_{n=1}^{N_{PT \max}} M_i[n] e^{-\frac{M_i}{R} p_n} \leq N_{UL} \\ M_i[n] \left(1 - \frac{p^n}{\sum_{n=1}^{N_{PT \max}} M_i[n] p^n} \right) N_{UL} & \text{otherwise} \end{cases} \quad (6)$$

If $n > 1$, the total number at the n -th RA attempt, $M_i[n]$, of UE of the i -th RA timeslot can be approximately written as Eq. (7), where $M_{k,F}[n-1]$ denotes the $(n-1)$ -th preamble transmitted by UE at the k -th RA timeslot but in vain. The $\alpha_{k,I}$ of UE suffering from the above failure is retransmitted in the i -th RA timeslot. K_{\min} and K_{\max} represent the minimum and maximum of k , respectively.

$$M_i[n] \approx \sum_{k=K_{\min}}^{K_{\max}} \alpha_{k,I} M_{k,F}[n-1] \quad \text{if } n > 1 \quad (7)$$

In Eq. (7), the upper limit, K_{\max} , and the lower limit, K_{\min} , of the transmission probability, $\alpha_{k,I}$, can be derived by the sequence chart from Literature [8]. K_{\max} and K_{\min} are given by Eq. (8) and Eq. (9), respectively. If the backoff interval of the k -th RA is overlapped with the transmitting interval of the i -th RA timeslot, then the UE failing to transmit the preamble at the k -th RA timeslot will retransmit a new preamble at the i -th RA. Therefore, $\alpha_{k,I}$ denotes the backoff interval of the k -th RA interval, whose transmission interval is overlapped with that of the i -th RA timeslot ($k < i$). At $(k-1)T_{RA_REP}$, the UE transmitting its preamble at the k RA timeslot will recognize the RA fault after the $(T_{RAR} + W_{RAR})$ subframe. Every UE failing to send the preamble will launch its backoff at the time of “ $(k-1)T_{RA_REP} + (T_{RAR} + W_{RAR}) + 1$ ”. Therefore, the backoff interval at the k -th RA timeslot starts at “ $(k-1)T_{RA_REP} + T_{RAR} + W_{RAR} + 1$ ” and ends at “ $(k-1)T_{RA_REP} + (T_{RAR} + W_{RAR}) + W_{BO}$ ”. If their backoff fills in between the $(i-1)$ th RA timeslot and the i -th RA timeslot, then the UE can upload the preambles at the i -th RA timeslot. Therefore, the transmission interval of the i -th RA can be written as “[$(i-1)T_{RA_REP} + 1(i-1)T_{RA_REP}$]”.

When the right boundary of the backoff interval at the k -th RA timeslot arrives at the left boundary of the transmission interval at the i -th RA timeslot, namely “ $(K_{\min} - 1)T_{RA_REP} + T_{RAR} + W_{RAR} + W_{BO} \geq 1 + (i-2)T_{RA_REP}$ ”, then K_{\min} can be obtained, and written as below:

$$K_{\min} = \left\lceil (i-1) + \frac{1 - (T_{RAR} + W_{RAR} + W_{BO})}{T_{RA_REP}} \right\rceil \quad (8)$$

When the left boundary of the backoff interval at the k -th RA timeslot arrives at the right boundary of the transmission interval at i -th RA timeslot, namely “ $(K_{\max} - 1)T_{RA_REP} + T_{RAR} + W_{RAR} + 1 \leq (i-2)T_{RA_REP}$ ”, then $k(K_{\max})$ can be obtained, and written as below:

$$K_{\max} = \left\lfloor i - \frac{1 + (T_{RAR} + W_{RAR})}{T_{RA_REP}} \right\rfloor \quad (9)$$

3 Performance Indexes

As mentioned above, performance indexes of the analysis model based on the pre-backoff group paging mechanism include: (1) Probability of conflict (P_C); (2) Probability of successful access (P_S); and (3) Delay of average access (D_A).

Among them, probability of conflict (P_C) is defined as the ratio of the number of preambles with collision conflicts and the number of all preambles; probability of successful access (P_S) is defined as the ratio of the number of UE with success network access to the total number of UE accessing within the timeslot; delay of average access (D_A) is defined as the period of time from the start of access upon paging to the establishment of network connection after completion of four steps of random access. Delay normalization is conducted of all UE with successful access will undergo obtain the delay of average access, D_A [9, 10].

Literature [6] provides the definition for formulas and parameters, including P_C , P_S and D_A , and these three performance indexes can be given by Eq. (10), Eq. (11), and Eq. (12), respectively.

$$P_C = \frac{\sum_{i=1}^{Imax} (R - M_i e^{-\frac{M_i}{R}} - R e^{-\frac{M_i}{R}})}{ImaxR} \tag{10}$$

$$P_S = \frac{\sum_{i=1}^{Imax} \sum_{n=1}^{NPTmax} M_{i,s}[n]}{M} \tag{11}$$

$$D_A = \frac{\sum_{i=1}^{Imax} \sum_{n=1}^{NPTmax} M_{i,s}[n] T_i}{\sum_{i=1}^{Imax} \sum_{n=1}^{NPTmax} M_{i,s}[n]} \tag{12}$$

Where, T_i denotes the access delay of UE with successful access via preamble transmission within the RA timeslot, which can be obtained through Eq. (13):

$$T_i = (i - 1)T_{RA_REP} + T_{RAR} + W_{RAR} \tag{13}$$

Of special note is that a high P_S , a low P_C , and a low D_A can be chosen as the desired results. The larger the backoff window, W_{PBO} , is, the lower the probability of conflict, P_C , is, and the higher the probability of successful access, P_S , is, namely the better the effects of users' access to the RCA. However, if the pre-backoff window changes, the delay of average access, D_A , of users will change as well. Therefore, it is necessary to find a suitable value for the backoff window, W_{PBO} .

4 Simulation Results and Discussions

By analyzing MATLAB simulation results of the probability of conflict (P_C), successful access probability (P_S) and delay of average access (D_A), this paper verifies the effectiveness of the pre-backoff group paging mechanism.

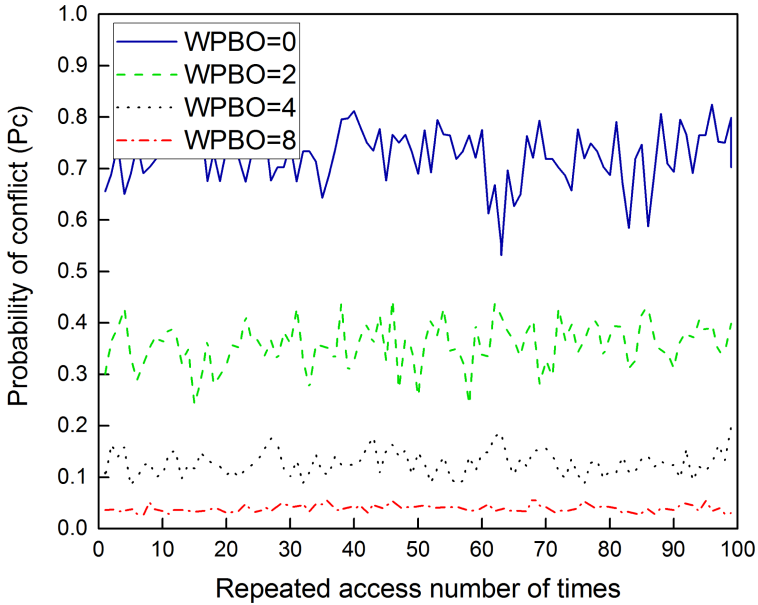


Fig. 1. Probability of conflict, P_C (Color figure online)

Currently, there have not yet been any suitable scenarios which can be used to compare the performance of the RAN (Radio Access Network) overload control plan based on the push and pull media. So, this paper compares the group paging strategies with other push plans. The simulation results of the pre-backoff group paging mechanism is shown in Fig. 1, Fig. 2, and Fig. 3. The numerical results are expressed by dots, and results of 100 repeated random access are adopted for analysis and discussion.

4.1 Charts of Simulation Results

Figure 1 presents the simulation results of probability of conflict (P_C), which shows the probability of conflict of every access of 160 pieces of UE in the group with repeated access to the RCH for 100 times, when the pre-backoff window, W_{PBO} , is set to different values. The blue full line in Fig. 1 denotes the probability of conflict when $W_{PBO} = 0$, namely the probability of conflict (P_C) of all UE receiving paging information from certain group and with direct access to the RCH within the RA timeslot. From Fig. 1, it can be seen that the probability of conflict, at $W_{PBO} = 0$ changes within the range of 0.5 to 0.85, so the ratio of the number of preambles with collision conflicts to the number of all preambles during the process of random access is very high, which might cause serious congestion. In Fig. 1, the green imaginary line represents the probability of conflict when $W_{PBO} = 2$. All the 160 users within the group are evenly distributed within two RA timeslots for random access. When P_C is fluctuating within the range of 0.2–0.45, the probability of conflict significantly declines compared with direct access without the introduction of pre-backoff. The black imaginary line represents the probability of conflict when $W_{PBO} = 4$. The 160 pieces of UE are evenly distributed within four

RA timeslots via pre-backoff for random access, and P_C fluctuates within the range of 0.08–0.20. As the value of the pre-backoff window, W_{PBO} , increases, the probability of conflict, P_C , keeps on declining. The red imaginary line represents the probability of conflict (P_C) when $W_{PBO} = 8$. All the 160 pieces of UE are evenly distributed within eight RA timeslots for random access through pre-backoff. P_C fluctuates within the range of 0.02–0.06. When the pre-backoff window, W_{PBO} , is set to be its maximum, 8, the probability of conflict, P_C , turns out to be the minimum.

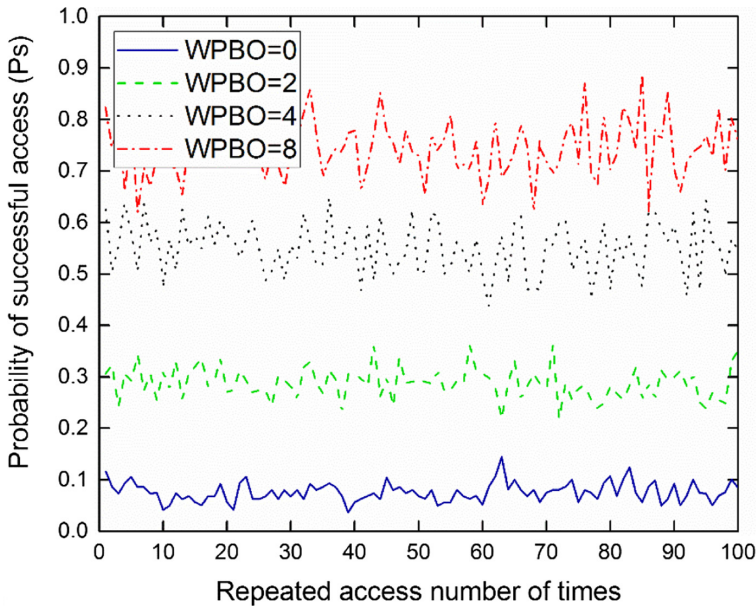


Fig. 2. Successful access probability, P_S (Color figure online)

Figure 2 shows the simulation results of probability of successful access (P_S), where the blue solid line represents the probability of successful access (P_S) when $W_{PBO} = 0$, namely the probability of successful access when all UE receiving paging messages from certain group has direct access to the RCH within the RA timeslot. From Fig. 2, one can observe that the probability of successful access (P_S) when $W_{PBO} = 0$ fluctuates within the range of 0.03–0.15. Therefore, the ratio of the number of UE with successful network access to the total number of UE accessing within the timeslot is very slow, which is obviously not the desired result. During the process of random access, as many pieces of UE receiving paging messages as possible are expected to realize successful network access. The green imaginary line represents the probability of success access (P_S). The 160 pieces of UE within the group are evenly distributed within two RA timeslots for random access via pre-backoff. When P_C is fluctuating within the range of 0.2–0.4, the probability of successful access (P_S), compared with direct access without introducing pre-backoff, obviously increases. The black imaginary line represents the probability of successful access (P_S) when $W_{PBO} = 4$, and P_S fluctuates within the range of 0.4–0.7. As the value of the pre-backoff window, W_{PBO} , increases, the successful access probability,

P_S , continues rising. The red solid line represents the probability of successful access (P_S) when $W_{PBO} = 8$, and P_S fluctuates within the range of 0.6–0.9. When the value of the pre-backoff window, W_{PBO} , is set to be the maximum, 8, the probability of successful access (P_S) turns out to be the maximum.

Figure 3 displays the simulation results of the delay of average access (D_A). Access delay refers to the period of time from the start of access upon paging to the establishment of network connection after completion of four steps of random access. Delay normalization is conducted of all UE with successful access to obtain the delay of average access, D_A . The blue solid line represents the delay of average access, D_A , when $W_{PBO} = 0$. D_A fluctuates around the 7.5 sub-frame. In random access, a low probability of conflict (P_C), a high probability of successful access (P_S), and a low delay of average access (D_A) are desired. The green imaginary line represents the delay of average access (D_A) when $W_{PBO} = 2$. All the 160 pieces of UE within the group are evenly distributed within two RA timeslots for random access via pre-backoff. D_A fluctuates around the 5.8 sub-frame. The delay of average access (D_A), compared with that of direct access without introducing pre-backoff, significantly declines. The black imaginary line represents the delay of average access (D_A) when $W_{PBO} = 4$, and D_A fluctuates around the 5.0 sub-frame. As the value of the pre-backoff window, W_{PBO} , increases, the delay of average access (D_A) decreases slightly. The red solid line represents the delay of average access (D_A) when $W_{PBO} = 8$. D_A fluctuates around the 6.3 sub-frame. As the value of the pre-backoff window (W_{PBO}) increases, the delay of average access (D_A) increases to the contrary.

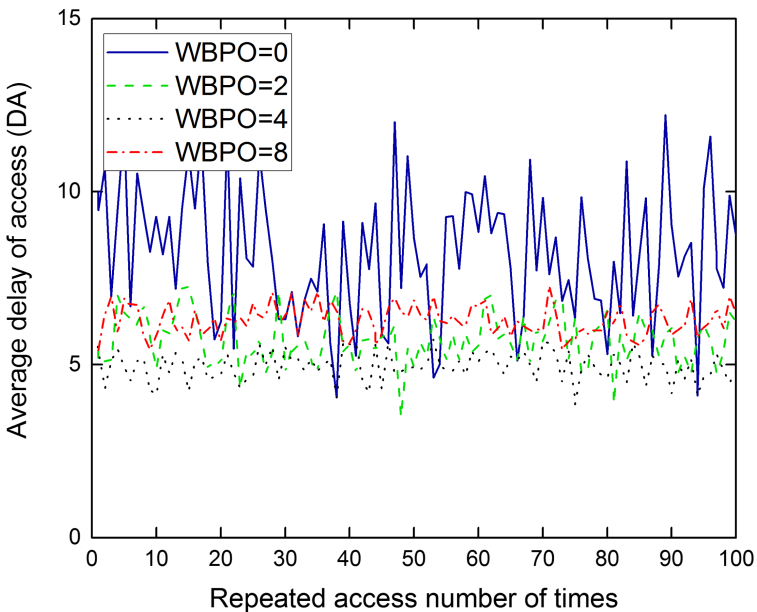


Fig. 3. Delay of average access, D_A (Color figure online)

Figure 4 presents the average probability of conflict (P_C) and probability of successful access (P_S) at different numbers of UE with network access. The asterisk indicates the average probability of conflict (P_C) and the circle indicates the average probability of successful access (P_S), both at different numbers of UE with network access. It can be clearly seen that, without pre-backoff, the number of UE is 160 and, at the moment, the probability of conflict (P_C) is the highest, while the probability of successful access (P_S) is the lowest, which suggests serious congestion. With the increasing number of pre-backoff windows (W_{PBO}), namely when the number of UE accessing at the same RA timeslot, the probability of conflict (P_C) keeps on declining, while the probability of successful access (P_S) keeps on increasing. This means that the competition conflict resulted from concentrated user access to the network during the process of group paging is satisfactorily improved.

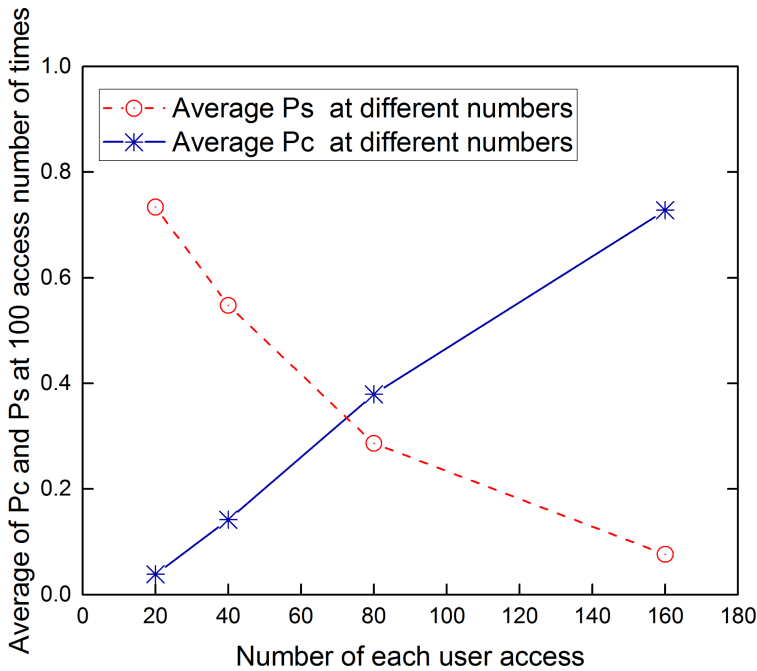


Fig. 4. Average P_C and P_S at different numbers of UE with network access

4.2 Simulation Results and Discussions

The simulation results of Fig. 1, Fig. 2, and Fig. 3 consider the situation when the pre-backoff window, W_{PBO} , is set to be 0, 2, 4 and 8, respectively. During the process of simulation, the group size, M , is set to be 160. Figure 1, Fig. 2 and Fig. 3 demonstrate the simulation results of the probability of conflict (P_C), probability of successful access (P_S), and delay of average access (D_A). The overall simulation results imply that the

analysis model can relatively accurately estimate the performance of the pre-backoff group paging mechanism at different values of W_{PBO} . In Fig. 1, the probability of conflict (P_C) decreases as W_{PBO} increases. When the value of W_{PBO} reaches the maximum, the minimum of P_C is obtained. Simulation results also suggest that, as the value of W_{PBO} increases, the probability of conflict of the pre-backoff paging conflict keeps on decreasing. This is because the pre-backoff mechanism will expand the access of UE at the first RA timeslot to the even access of UE at multiple RA timeslots. In Fig. 2, the probability of successful access (P_S) increases as the value of W_{PBO} increases, and P_S reaches its maximum when the W_{PBO} is at its maximum. Simulation results mean that, as the value of W_{PBO} increases, the probability of successful access based on the pre-backoff group paging mechanism keeps on rising. In Fig. 3, the delay of average access, D_A , first increase and then decrease, as the value of W_{PBO} increase. Simulation results provide solid evidence for that the pre-backoff group paging mechanism can significantly increase the probability of successful access, and also maintain a low delay of average access for UE with successful access. In Fig. 4, the average probability of conflict (P_C) and the average probability of successful access (P_S), both at different numbers of UE, are compared. As the number of UE accessing within the same RA timeslot decreases, the probability of conflict (P_C) keeps on decreasing, while the probability of successful access (P_S) keeps on rising. To sum up, the above simulation results can verify the validity of the group paging mechanism analysis model with the pre-backoff algorithm introduced, in that, the analysis model can favorably improve the competition conflict resulted from users' concentrated access to the network, and also satisfy the requirement of overload control.

5 Conclusions

All in all, this paper proposes the pre-backoff group paging mechanism as a solution plan for congestion caused by MTC random access. Simulation results suggest that, when the group size is large, the pre-backoff method can significantly improve the performance of the group paging strategy, alleviate the competition conflict resulted from UE's concentrated access to the network, and satisfy users' requirement of access QoS.

Acknowledgment. This work was supported by the Beijing City Board of education project (NO. KM202010858005).

References

1. Xian-Feng, W., Yin-Feng, W.: Study on M2M based on PLMN. *Commun. Tech.* **40**(3), 66–68 (2012)
2. Dapeng, W., Hang, S., Honggang, W., et al.: A feature based learning system for internet of things applications. *IEEE Internet Things J.* **6**(2), 1928–1937 (2019)
3. Zhang, H., Huang, S., Jiang, C., et al.: Energy efficient user association and power allocation in millimeter wave based ultra dense networks with energy harvesting base stations. *IEEE J. Sel. Areas Commun.* **35**(9), 1936–1947 (2017)

4. Zhang, H., Dong, Y., Cheng, J., et al.: Fronthauling for 5G LTE-U ultra dense cloud small cell networks. *IEEE Wirel. Commun.* **23**(6), 48–53 (2017)
5. Dapeng, W., Qianru, L., Honggang, W., et al.: Socially aware energy-efficient mobile edge collaboration for video distribution. *IEEE Trans. Multimedia* **19**(10), 2197–2209 (2017)
6. Jiang, W., Wang, X.: Group paging based on pre-backoff access scheme in Machine-type Communications. *Commun. Tech.* **47**(2), 172–178 (2014)
7. Wei, C.-H., Cheng, R.-G., Tsao, S.-L.: Performance analysis of group paging for machine-type communications in LTE networks. *IEEE Trans. Veh. Tech.* **62**(7), 3371–3382 (2013)
8. Farhadi, G., Ito, A.: Group-based signaling and access control for cellular machine-to-machine communication. In: *Vehicular Technology Conference*, pp. 1–6. IEEE, Las Vegas (2013)
9. Chen, Yu., Guo, Z., Yang, X., Hu, Y., Zhu, Q.: Optimization of coverage in 5G self-organizing small cell networks. *Mob. Netw. Appl.* **23**(6), 1502–1512 (2017). <https://doi.org/10.1007/s11036-017-0983-x>
10. Dapeng, W., Zhihao, Z., Shaoen, W., et al.: Biologically inspired resource allocation for network slices in 5G-enabled internet of things. *IEEE Internet Things J.* 1, (2018). At present Online publishing